Journal of Catalysis 287 (2012) 203–209

Contents lists available at SciVerse ScienceDirect

Journal of Catalysis

journal homepage: www.elsevier.com/locate/jcat

Effects of hydrothermal aging on NH_3-SCR reaction over Cu/zeolites

Ja Hun Kwak *, Diana Tran, Sarah D. Burton, János Szanyi, Jong H. Lee *, Charles H.F. Peden *

Institute for Integrated Catalysis, Pacific Northwest National Laboratory, Richland, WA 99352, USA

ARTICLE INFO

Article history:
Received 1 August 2011
Revised 14 November 2011
Accepted 31 December 2011
Available online 31 January 2012

Keywords:
Cu-SSZ-13
NH_3-SCR
Hydrothermal aging
H_2-TPR
Solid state ^{27}Al NMR

ABSTRACT

The effects of hydrothermal treatment on model Cu/zeolite catalysts were investigated to better understand the nature of Cu species for the selective catalytic reduction of NO_x by NH_3. After hydrothermal aging at 800 °C for 16 h, the NO_x reduction performance of Cu-ZSM-5 and Cu-beta was significantly reduced at low temperatures, while that of Cu-SSZ-13 was not affected. When the zeolite framework aluminum species were probed using solid state ^{27}Al MASNMR, significant reduction in the intensities of the tetrahedral aluminum peak intensity was observed for Cu-ZSM-5 and Cu-beta, although no increase in the intensities of the octahedral aluminum peak was detected. When the redox behavior of Cu species was examined using H_2-TPR, it was found that Cu^{2+} could be reduced to Cu^+ and to Cu^0 for Cu-ZSM-5 and Cu-beta catalysts, while Cu^{2+} could be reduced only to Cu^+ in Cu-SSZ-13. After hydrothermal aging, CuO and Cu-aluminate species were found to form in Cu-ZSM-5 and Cu-beta, while little changes were observed for Cu-SSZ-13.

1. Introduction

Various catalyst technologies have been developed to remove pollutants from engine exhaust. For example, a three-way catalyst (TWC) is used to remove hydrocarbons (HC), carbon monoxide (CO), and nitrogen oxides (NO_x) from stoichiometric gasoline engines. For diesel engines, a diesel oxidation catalyst (DOC) is used to control HC and CO emissions, while particulate matters (PM) are removed by a diesel particulate filter (DPF). NO_x can be removed by either a lean NO_x trap (LNT) catalyst that can store NO_x under lean conditions and reduce NO_x under rich conditions, or by a selective catalytic reduction (SCR) catalyst that can selectively reduce NO_x with a reducing agent (e.g., NH_3, hydrocarbons) under oxidizing conditions. A typical emission control system for diesel engines consists of DOC, SCR, and DPF, which are placed in a specific order to achieve a desired level of emission reduction performance. As soot is often removed from the DPF at high temperatures (>650 °C), high thermal durability is required for the SCR catalyst to remain effective for NO_x emission control [1].

Among the various catalysts developed for NH_3 SCR, zeolite-based base metal (e.g., Cu, Fe) catalysts are currently being used for meeting diesel NO_x emission standards in North America. Significant research efforts have concentrated on Cu^{2+} ion-exchanged ZSM-5 (Cu-ZSM-5) zeolites to study both its NO decomposition and SCR activity [2]. Early development efforts have also focused on Cu^{2+} exchanged beta zeolite (Cu-beta) for its excellent activity over a wide range of temperatures. However, these catalysts have been found to deactivate readily during high-temperature filter regeneration. Recently, we reported that Cu^{2+} ion-exchanged SSZ-13 (Cu-SSZ-13), a zeolite with the Chabazite (CHA) structure and containing small radius (~3.8 Å) eight-membered ring pores, is more active and selective in reducing NO with NH_3 compared to Cu-ZSM-5 and Cu-beta [3].

It was also found that Cu-SSZ-13 is less prone to deactivation by hydrocarbon inhibition or thermal degradation [4,5]. Interestingly, some improvement in high-temperature activity has also been previously reported for some Cu/zeolite catalysts after hydrothermal aging, which may suggest that activity can sometimes improve during hydrothermal aging processes before the catalyst becomes fully deactivated [6]. Thus, in order to better understand the origin of high activity and thermal stability of Cu-SSZ-13, we investigate here the effects of high-temperature hydrothermal treatment on Cu species and zeolite framework structure, and on NO reduction activity using model Cu/zeolite catalysts, namely, Cu-SSZ-13, Cu-beta, Cu-ZSM-5, and Cu-Y.

2. Experimental

2.1. Catalyst preparation

ZSM-5 (CBV-3024, $Si/Al_2 = 30$), beta (CP-814C, $Si/Al_2 = 38$), and Y (CBV-100, $Si/Al_2 = 5.2$) zeolites were obtained from Zeolyst International Co. SSZ-13 ($Si/Al_2 = 12$) was prepared using the method reported previously [3,7]. Cu/zeolite catalysts were prepared by aqueous ion exchange using $Cu(NO_3)_2$ as precursor. Cu solutions contained twice the amount of Cu^{2+} ions needed for complete ion

---

* Corresponding authors.
E-mail addresses: kwak@pnnl.gov (J.H. Kwak), jong.lee@pnnl.gov (J.H. Lee), chuck.peden@pnnl.gov (C.H.F. Peden).

0021-9517/$ - see front matter © 2012 Elsevier Inc. All rights reserved.
doi:10.1016/j.jcat.2011.12.025

exchange. After ion exchange over 1 day at room temperature, the catalyst samples were filtered, washed, and dried overnight at 100 °C. In order to maximize the ion exchange level under the given experimental conditions, this entire process was repeated twice for each catalyst sample. The results of elemental analysis (ICP) for the thus prepared samples are summarized in Table 1. All catalysts were then calcined in an oven at 500 °C for 2 h prior to testing and characterization. For the hydrothermal aging studies, some of the catalysts were further treated in 10% H_2O in air at 800 °C for 16 h.

2.2. Catalytic activity measurement

Catalytic activity was measured using a packed bed micro reactor system. Catalyst samples (~250 mg) of 60–80 mesh size were loaded in a 3/8″ OD quartz tube, which was then placed inside an electric furnace. The reaction temperature was monitored by a thermocouple located at the inlet position. The feed gas contained 350 ppm NO_x, 350 ppm NH_3, 14% O_2, 10% H_2O, and balance N_2. All the lines were heated to over 100 °C to avoid condensation inside the reactor system. The total gas flow rate was 210 ml/min (STP), and the gas hourly space velocity (GHSV) was estimated to be ~30,000 h^{-1}. Concentrations of reactants and products were measured by a Nicolet Magna 760 infrared (FT-IR) spectrometer with a heated 2-m gas cell.

The catalysts were evaluated for their activity for NO_x reduction to N_2, and for NH_3 oxidation. The NO_x and NH_3 conversion efficiencies were calculated based on the differences in their concentrations measured before and after the catalyst in the following way:

$$\%\ NO_x\ \text{conversion} = \{(NO + NO_2)_{\text{inlet}} - (NO + NO_2 + 2^{*}N_2O)_{\text{outlet}}\}/(NO + NO_2)_{\text{inlet}} * 100$$

$$\%\ NH_3\ \text{conversion} = (NH_{3\text{inlet}} - NH_{3\text{outlet}})/NH_{3\text{inlet}} * 100$$

Note that for calculating NO_x conversions, N_2O is not considered to be a product, but rather unconverted NO_x.

2.3. Catalyst characterization

X-ray diffraction (XRD) measurements were made on a Philips PW3040/00 X'Pert powder X-ray diffractometer using Cu Kα radiation (λ = 1.5406 Å), with scans run between 2θ values of 5° and 50° at 0.02°/s. Diffraction patterns were analyzed using JADE (Materials Data, Inc.) as well as the Powder Diffraction File database (International Center for Diffraction Data, 2003 release).

Solid state ^{27}Al nuclear magnetic resonance (NMR) spectra were acquired on a Varian Chemagnetics CMX Infinity 300 MHz instrument, equipped with a Varian Chemagnetics 7.5 mm HX magic angle spinning (MAS) probe operating at the spectral frequency of 78.2 MHz. About 0.2 g of each catalyst sample was transferred into a gastight rotor (7.5 mm OD), which was then promptly placed in the probe and NMR magnet. All ^{27}Al MAS NMR spectra were externally referenced to an aqueous solution of $Al(NO_3)_3$ at 0 ppm. All spectra were obtained at a sample spinning rate of 5 kHz and using 1 s recycle delay. For comparison of signal intensities, the same amount of sample was used and the same number of scans was acquired for each experiment. A 10° flip angle was used during the single pulse experiment to obtain quantitative spectra.

Table 1
ICP analysis results of the Cu ion-exchanged zeolite samples before hydrothermal aging.

	Cu-Y, FAU	Cu-beta	Cu-ZSM-5	Cu-SSZ-13
Si/Al_2	5.3	39.0	32.9	12.4
Cu/Al	0.35	0.34	0.53	0.40
Cu loading (wt.%)	7.2	1.73	2.83	4.3
Cu I.E. level (%)	70	69	106	79

Prior to H_2 temperature-programmed reduction (TPR) experiments, 0.05 g of Cu–zeolite catalyst was calcined at 500 °C for 2 h in flowing air (1.0 ml/s). The sample was then cooled down to room temperature in the same air flow, and then purged in 2% H_2/Ar (1.0 ml/s) for 1 h at RT. Once the TCD signal of a Hewlett–Packard 7820 gas chromatograph (GC) stabilized, a TPR experiment was carried out in 2% H_2/Ar (1.0 ml/s) at a heating rate of 10 K/min. The amount of H_2 consumed was determined from TCD signal intensities, which were calibrated using a 10% CuO/SiO_2 reference sample.

3. Results and discussion

3.1. Catalyst activity measurements

The NO_x reduction activity of each Cu ion-exchanged zeolite catalyst was examined using the feed gas containing 350 ppm NO_x, 350 ppm NH_3, 14% O_2, and 10% H_2O at the GHSV of 30,000 h^{-1} between 150 and 550 °C. As shown in Fig. 1a, excellent NO reduction activity was obtained for all fresh Cu/zeolite catalysts. For example, NO reduction activity increased with increasing temperature, reaching 85–95% at 250 °C. At higher temperatures, NO reduction activity was limited by the availability of ammonia as the ammonia oxidation reaction to NO_x becomes significant. Interestingly, a significant amount of N_2O was produced over Cu-Y (shown in Fig. 2a). Because N_2O is a greenhouse gas, it is

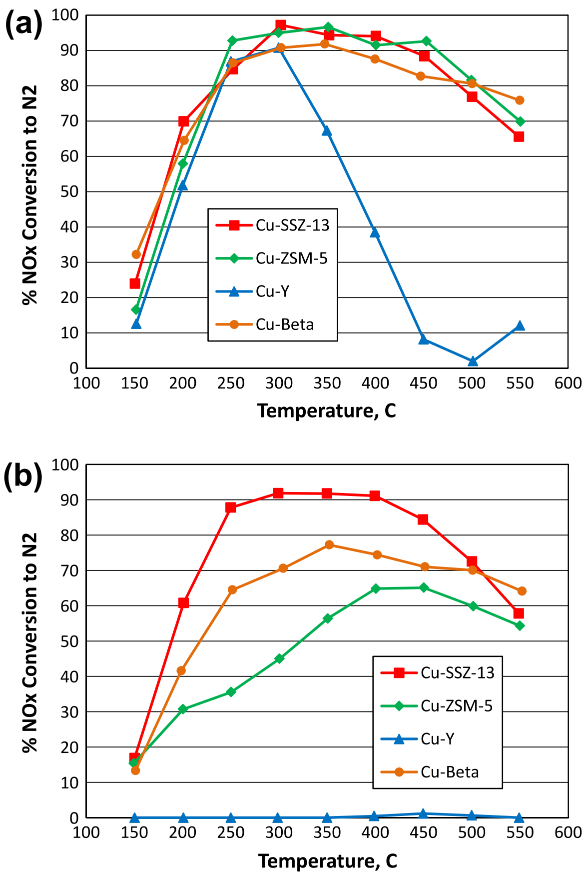

Fig. 1. NO conversion to N_2 over Cu/zeolites (a) fresh catalysts and (b) after hydrothermal aging (Feed: 350 ppm NO, 350 ppm NH_3, 14% O_2, 10% H_2O in balance N_2).

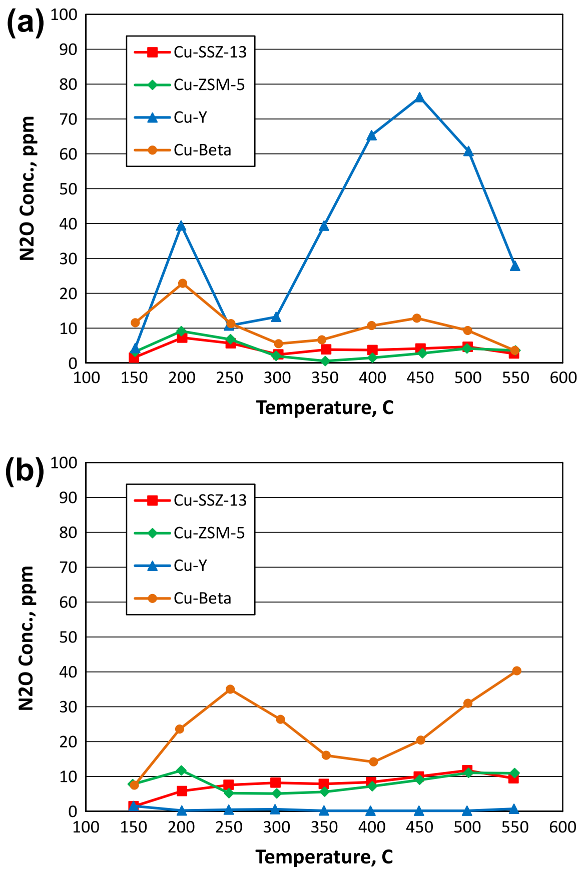

Fig. 2. N_2O formation over Cu/zeolites (a) fresh catalysts and (b) after hydrothermal aging (feed: 350 ppm NO, 350 ppm NH_3, 14% O_2, 10% H_2O in balance N_2).

not considered to be a desirable product. Thus, when N_2 was considered as the only product for the SCR reaction, very little NO reduction activity was seen for fresh Cu-Y at temperatures >350 °C. These results are consistent with our previous findings that showed high NO_x reduction activities for Cu ion-exchanged ZSM-5, beta, and SSZ-13 zeolites [3].

As mentioned earlier, SCR catalysts are often exposed to very high temperatures (>650 °C) during, for example, soot oxidation processes in upstream DPFs. As such, high hydrothermal durability is essential for practical implementation of the NH_3 SCR technology. To probe hydrothermal stability, the Cu/zeolite catalysts were further treated in 10% H_2O in air at 800 °C for 16 h to investigate the effects of hydrothermal aging on the catalytic activities and the catalyst structures. After this hydrothermal treatment, significant loss of NO reduction activity, in greatly varying extent, was observed for most of the Cu/zeolite catalysts (shown in Fig. 1b). While Cu-SSZ-13 was found to show essentially no change in NO reduction activity, Cu-Y lost its activity completely. Both Cu-ZSM-5 and Cu-beta were found to lose NO reduction activity primarily at low catalyst bed temperatures, but maintain reasonable activity at high (>350 °C) temperatures. Since these Cu/zeolite catalysts contain different amounts of Cu ions, turnover rates were estimated based on the amount of Cu present in the sample. As shown in Table 2, the loss of low-temperature NO reduction activity in high-temperature aged samples can be clearly observed for all Cu/zeolite catalysts, except Cu-SSZ-13. The amount of N_2O produced was low over all aged Cu zeolites, except Cu-beta (shown in Fig. 2b). In fact, N_2O formation over the aged Cu-beta was much higher than on the fresh Cu-beta at all temperatures.

Table 2
Turnover rates of Cu ion-exchanged zeolite samples before and after hydrothermal aging.

Samples	Turnover rate (/s)*	
	150 °C	200 °C
Cu-Y		
Fresh	2.23×10^{-3}	1.18×10^{-2}
HTA	0	0
Cu-beta		
Fresh	3.69×10^{-2}	7.36×10^{-2}
HTA	1.74×10^{-2}	5.24×10^{-2}
Cu-ZSM-5		
Fresh	1.32×10^{-2}	2.87×10^{-2}
HTA	1.12×10^{-2}	2.13×10^{-2}
Cu-SSZ-13		
Fresh	7.60×10^{-3}	2.30×10^{-2}
HTA	7.60×10^{-3}	2.88×10^{-2}

* Estimated based on the number of Cu ions.

Data in Figs. 1 and 2 were for reaction mixtures that contained NO_x entirely in the form of NO (the so-called "standard" SCR reaction). However, it is well known that NH_3 SCR reaction kinetics can be improved in the presence of equimolar amounts of NO and NO_2 in the feed gas via the "fast" SCR reaction [8]. For this reason, a typical emission control system for diesel engines often includes a DOC ahead of the SCR catalyst to convert some of the exhaust NO to NO_2 [1]. However, when NO_2 is included in the feed, N_2O is often produced at higher levels via a reaction mechanism that involves the catalyzed formation and decomposition of NH_4NO_3 [9]. As shown in Fig. 3, various amounts of N_2O were obtained over both fresh and aged Cu/zeolite catalysts under the conditions used in

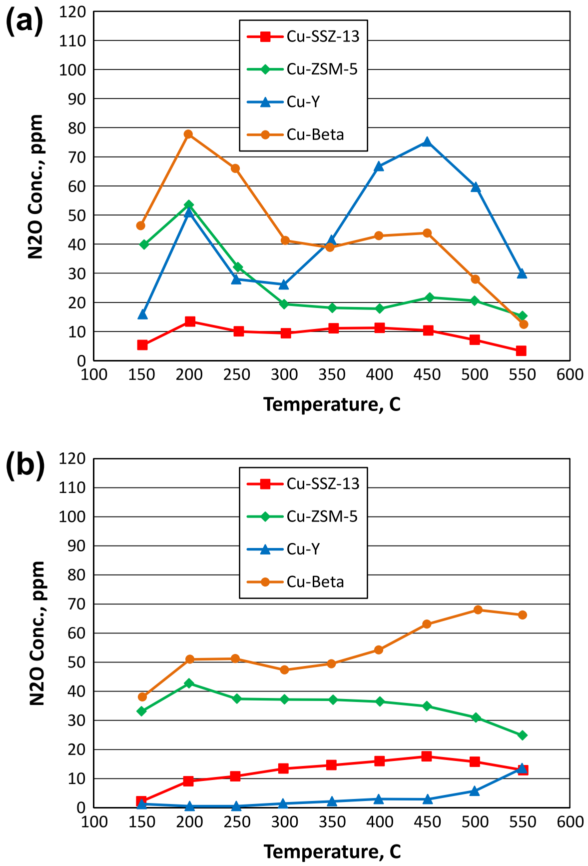

Fig. 3. N_2O formation over Cu/zeolites (a) fresh catalysts and (b) after hydrothermal aging (feed: 175 ppm NO, 175 ppm NO_2, 350 ppm NH_3, 14% O_2, 10% H_2O in balance N_2).

this study. Interestingly, Cu-SSZ-13 was found to reduce NO_x to N_2 almost exclusively even in the presence of NO_2. Because very little N_2O formation was seen over other small pore Cu/zeolite catalysts [5], it is possible that the observed high selectivity to N_2 may be related to the zeolite structure (type), and this aspect is currently under investigation.

Because of the enhanced NO_x reduction kinetics in gas mixtures containing equimolar NO/NO_2 (fast SCR), high NO_x reduction activity is typically reported for many of the Cu/zeolite catalysts, especially at lower temperatures. Note, however, that when only N_2 is considered as the N-containing reaction product (i.e., N_2O is still defined as NO_x), our results show that improved NO_x reduction activity is obtained for Cu-SSZ-13 only (Fig. 4a). Following the hydrothermal treatment at 800 °C for 16 h, some loss of NO_x reduction activity was observed in Cu-SSZ-13 at low and high temperatures (shown in Fig. 4b). On the other hand, total loss of activity was observed for Cu-Y, and both Cu-ZSM-5 and Cu-beta were found to lose NO_x reduction activity, in part because of increased N_2O formation following hydrothermal aging.

3.2. Catalyst characterization

Previously, adverse effects of hydrothermal aging on NO_x reduction activities of zeolite-based catalysts have been associated primarily with the degradation of the zeolite structure or the deactivation of catalytically active sites by cation migration [10]. In order to better understand the changes in the NO_x reduction activity induced by hydrothermal aging, changes in the physico-chemical properties of the Cu/zeolite catalysts were examined using XRD, ^{27}Al MAS NMR, and H_2-TPR techniques. In particular, degradation of the crystalline zeolite structure can be followed by powder XRD, while the removal of tetrahedral Al^{3+} ions from the zeolite framework (i.e., dealumination) can be monitored by ^{27}Al MAS NMR. On the other hand, changes in the chemical environment of the Cu ions may be reflected in their reducibilities as measured by H_2-TPR.

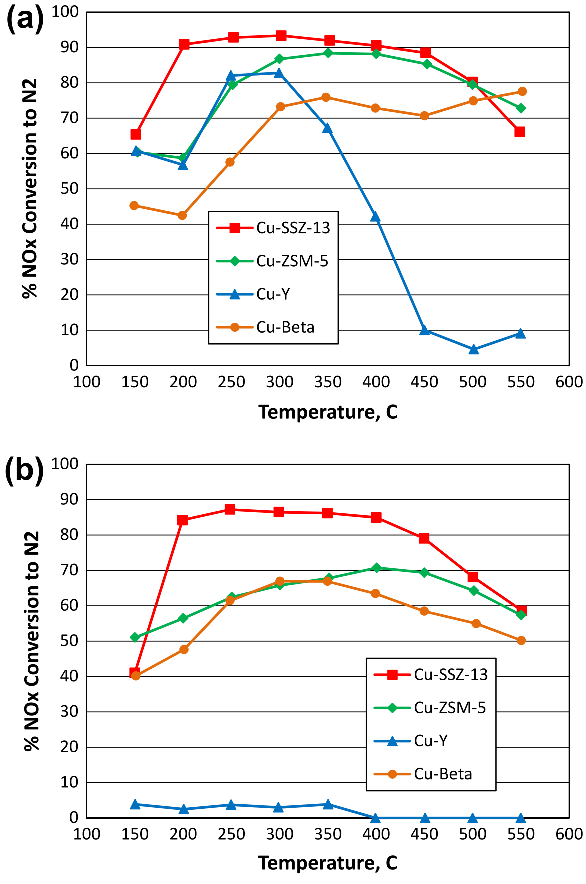

Fig. 4. NO_x conversion to N_2 over Cu/zeolites (a) fresh catalysts and (b) after hydrothermal aging (feed: 175 ppm NO, 175 ppm NO_2, 350 ppm NH_3, 14% O_2, 10% H_2O in balance N_2).

First, XRD measurements were performed over both fresh and aged samples to probe possible structural changes. XRD patterns recorded for the fresh (panel A) and hydrothermally aged (panel B) Cu/zeolite samples are displayed in Fig. 5. Comparison of the XRD patterns from the fresh and aged samples clearly show the complete collapse of the zeolite structure for Cu-Y as a result of hydrothermal aging, consistent with the total loss of its SCR activity. For this catalyst, instead of crystalline zeolite diffraction peaks, a broad feature representing an amorphous phase with CuO peaks is evident in the diffraction pattern following the hydrothermal aging. On the other hand, little or no changes were observed for Cu-SSZ-13, Cu-ZSM-5, and Cu-beta, which indicate that these zeolite structures remained largely intact during the hydrothermal aging. For these Cu/zeolite catalysts, despite some changes in SCR activity, no formation of CuO is evident in the XRD data.

Most zeolites can dealuminate under high-temperature hydrothermal conditions without exhibiting significant damage to their crystal structures. During this process, Al^{3+} ions are removed from their tetrahedral positions in the zeolite framework, and extra-framework AlO_x species can be produced. As the Al^{3+} in the AlO_x

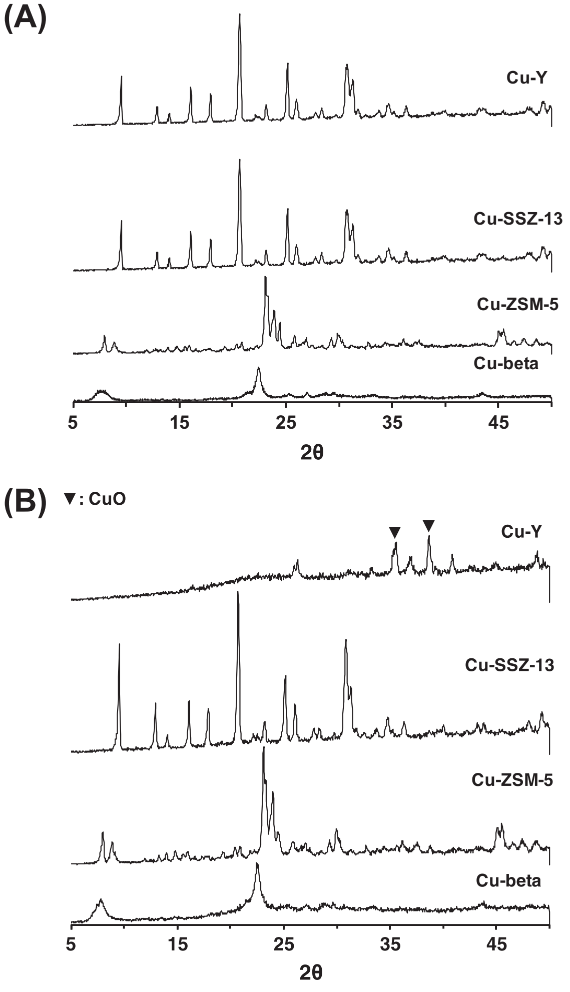

Fig. 5. XRD patterns of Cu/zeolites before (A) and after (B) hydrothermal aging.

species possesses octahedral coordination, the dealumination can be conveniently monitored by ^{27}Al MAS NMR [12–15] by a peak at ~0 ppm. For example, a decrease in the intensity of the tetrahedrally coordinated Al^{3+} ions and concurrent increase in the intensity of the octahedrally coordinated Al^{3+} ions are expected for dealuminated zeolite samples.

As shown in Fig. 6, all fresh Cu/zeolite catalysts show a single tetrahedral aluminum peak at ~50–60 ppm chemical shift range (e.g., Cu-ZSM-5 = 53 ppm, Cu-beta = 53 ppm, Cu-Y = 59 ppm, and Cu-SSZ-13 = 57 ppm). The peaks recorded for these Cu/zeolite catalysts are broader than those of Na-exchanged zeolites due to line broadening effects of paramagnetic Cu^{2+} ions. A broad peak at ~0 ppm appears to be due to either an artifact from the instrument or data processing, and less likely associated with octahedral aluminum ions in the fresh samples. Following the hydrothermal aging, the intensities of these tetrahedral aluminum signals were reduced significantly for three of the four zeolite samples studied, remaining mostly unchanged for Cu-SSZ-13. Compared to the fresh samples, the integrated peak areas of the tetrahedral Al^{3+} ions in the aged samples, which are proportional to the number of framework aluminum ions, were estimated to be only ~57% in Cu-ZSM-5, ~31% in Cu-beta, and ~23% in Cu-Y. In contrast, the peak area for aged Cu-SSZ-13 was very high, around 95% of the fresh sample. The observed high thermal stability for the Cu-SSZ-13 catalyst is consistent with the minor change in its SCR activity. It is well known that tetrahedral aluminum ions in the zeolite framework are changed to octahedral aluminum upon dealumination under high-temperature hydrothermal treatment. However, no new peaks associated with octahedral aluminum were observed in any of the samples used in this study. The lack of octahedral aluminum ions in the aged zeolite catalysts strongly suggests that paramagnetic Cu ions may interact more strongly with the forming octahedral aluminum than zeolytic Cu ions with framework aluminum.

H_2-TPR experiments were performed to examine the effects of hydrothermal aging on the nature of Cu species. As shown in Fig. 7, H_2-TPR spectra collected over fresh Cu/zeolites could be divided into two groups based on the reducibility of Cu ions. For fresh Cu-ZSM-5, three reduction peaks were observed at 155 °C, 207 °C, and 315 °C. In the literature, it was suggested that Cu^{2+} is reduced to Cu^{+} at ~200 °C, while Cu^{+} is reduced to Cu^{0} at 315 °C for Cu-ZSM-5 catalysts [10,11]. The observed peak at 155 °C peak may be a result of the reduction of oxygen in Cu–O–Cu structures, which can be formed at high Cu ion exchange levels (the elemental analysis results shown in Table 1 suggest that the Cu ion exchange level in our Cu-ZSM-5 sample slightly exceeds 100%, i.e., this sample is regarded as over-exchanged). Similar to Cu-ZSM-5, two reduction peaks were observed at 200 °C and 390 °C for Cu-beta, which can be attributed to the reduction of Cu^{2+} to Cu^{+}, and that of Cu^{+} to Cu^{0}, respectively. On the other hand, the two reduction peaks observed at 195 °C and 310 °C for Cu-Y catalysts are assigned only to the reduction of Cu^{2+} to Cu^{+} based on the literature, which suggested that Cu^{2+} ions inside supercages of faujasite (FAU) zeolites are reduced to Cu^{+} at 195 °C, while reduction of Cu^{2+} ions to Cu^{+} inside sodalite cages occurs at 310 °C [16].

Interestingly, only one H_2-TPR reduction peak at 230 °C with a broad shoulder at ~300 °C was obtained for Cu-SSZ-13. During the TPR, Cu-SSZ-13 appeared white even at 700 °C, which suggests the formation of Cu^{+}, a result consistent with those reported by Kieger et al. [16]. Notably, in this prior work, the authors report that the color of Cu-Y powders turned white due to Cu^{+} formation and then became purple when Cu^{+} was further reduced to Cu^{0} at higher temperatures. A purple color due to Cu^{0} formation was confirmed in the present work for Cu-beta and Cu-ZSM-5 after TPR up to 700 °C. Based on these results, we assign the 230 °C peak and 300 °C shoulder on Cu-SSZ-13 as both arising from Cu^{2+} to Cu^{+} reduction with different ionic positions in the zeolite structure.

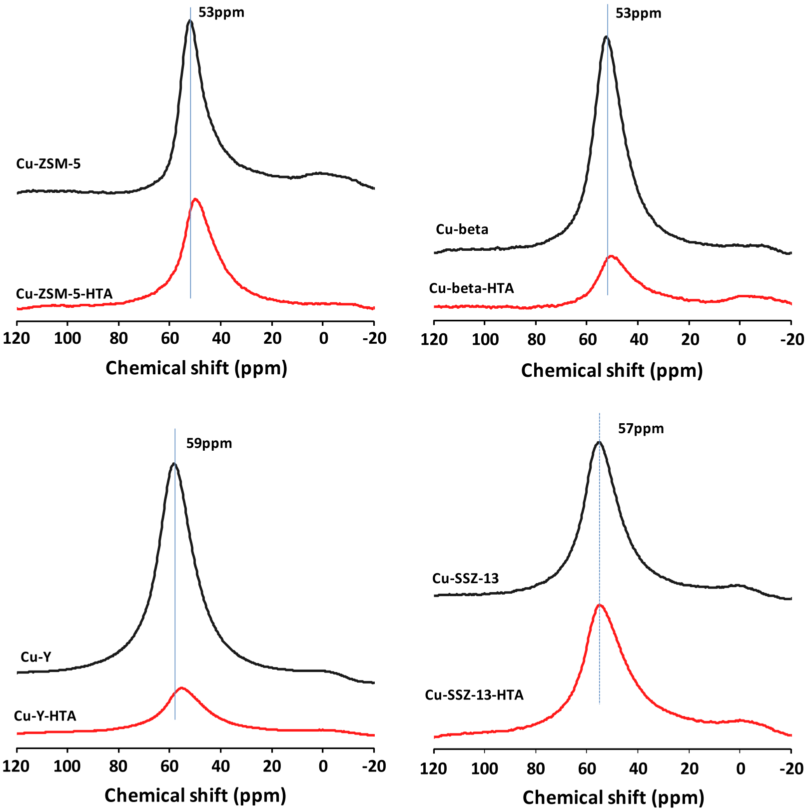

Fig. 6. Solid state ^{27}Al-NMR spectra of Cu/zeolites before and after hydrothermal aging.

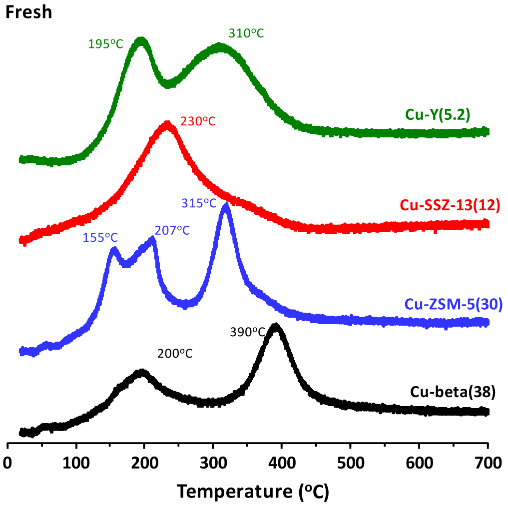

Fig. 7. H_2-TPR profiles of fresh prepared Cu/zeolites; Cu-beta (black), Cu-ZSM-5 (blue), Cu-SSZ-13 (red), and CuY (green). (For interpretation of the references to color in this figure legend, the reader is referred to the web version of this article.)

Recently, it was reported that there are several exchange sites inside chabazite (CHA) zeolites available for Cu ions [17]. Among them, it has been proposed that Cu cations can occupy two of these sites: "site I," located inside the CHA cavity, and "site IV," inside the eight-membered ring connecting the CHA cavities. Note that site I is similar to the exchange sites inside the sodalite cage of FAU zeolite where the Cu^{2+} to Cu^{+} reduction has been proposed to occur at ~300 °C. Based on these previous assignments, it seems reasonable to propose that the prominent H_2-TPR peak at 230 °C is due to the reduction of Cu^{2+} to Cu^{+} at the IV site, while the broad shoulder peak is perhaps due to Cu^{2+} to Cu^{+} reduction for Cu ions at site I. However, these assignments must be considered as tentative at best at this point, as they contradict the conclusion of Fickel and Lobo [7], who proposed the presence of Cu ions exclusively in one type of cationic positions. Current studies in our laboratory are aimed solely at understanding the locations of Cu ions in our in-house synthesized SSZ-13 sample.

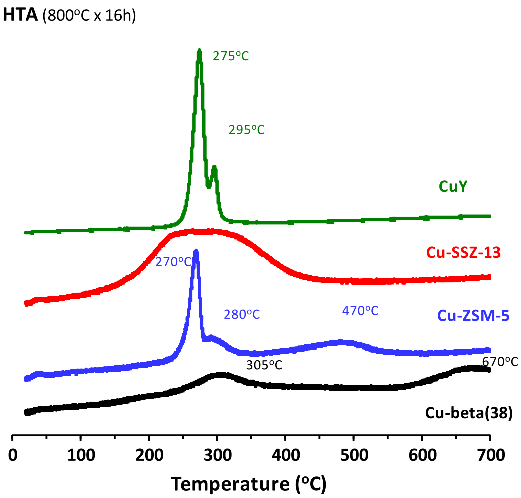

Fig. 8. H_2-TPR profiles of Cu/zeolites after hydrothermal aging; Cu-beta (black), Cu-ZSM-5 (blue), Cu-SSZ-13 (red), and CuY (green). (For interpretation of the references to colour in this figure legend, the reader is referred to the web version of this article.)

Following the hydrothermal aging at 800 °C, significant differences in the H_2-TPR patterns were observed, as shown in Fig. 8. For Cu-Y, sharp peaks at 275 and 295 °C are attributed to the reduction of bulk-like CuO structures formed during the total collapse of the zeolite structure. For Cu-beta, two broad reduction peaks are now present at 305 and 670 °C. As most of the zeolite structure was still intact after the hydrothermal aging, these H_2-TPR features may still be attributed to the reduction of Cu^{2+} and Cu^{+} ions. Over Cu-ZSM-5, a sharp reduction peak at 270 °C for bulk-like CuO is observed, as well as broad peaks at 280 and 470 °C, similar to those for Cu-beta. In trying to rationalize these changes, a couple of points are likely to be relevant. First, prior literature has reported that H_2-TPR reduction peaks are shifted to higher temperatures when the ion exchange level of Cu is decreased [18]. Furthermore, the NMR results described above indicate a moderate loss of Cu ions from the ion exchange sites for both Cu-beta and Cu-ZSM-5 catalysts with a subsequent formation of new Cu-aluminum-oxygen complexes where Cu strongly interacts with the Al ions, therefore rendering the ^{27}Al NMR peaks associated with these new complexes "invisible" in the spectra. Thus, the observed shift in peak temperatures and reduction in peak intensities may represent the reduced occupancy of the zeolite ion exchange sites by Cu and/or the reduction of Cu ions in the newly formed Cu-AlO_x species.

On the other hand, for Cu-SSZ-13, Fig. 8 shows that the reduction peak at 230 °C is still present and that the broad shoulder at ~300 °C has increased after hydrothermal aging. Furthermore, we find that essentially the same amount of H_2 is consumed for both the fresh and aged Cu-SSZ-13 samples, suggesting relatively small changes in the distribution of Cu ions between the likely two zeolytic sites in SSZ-13. This result is consistent with the small observed changes in both the solid state ^{27}Al NMR spectra and SCR activity for Cu-SSZ-13 catalysts after hydrothermal aging.

Considering the changes observed in ^{27}Al NMR and H_2-TPR, it is likely that some of the Cu^{2+} ions in aged Cu-ZSM-5 and Cu-beta are still located in ion exchange positions within zeolite structure and, thus, responsible for the SCR activity albeit severely suppressed. On the other hand, both aged Cu-ZSM-5 and Cu-beta exhibited relatively good NO_x reduction activity at higher temperatures. Recently, we demonstrated that isolated Cu species on γ-alumina can be effective in NH_3 SCR [19]. The somewhat different structures for Cu species in these alumina supported catalysts and Cu ions exchanged into zeolites likely explain the considerable differences in the optimum temperature ranges for NH_3 SCR activity for these two types of catalysts. Based on these recent results, we propose that new Cu/AlO_x structures that form upon hydrothermal aging and which exhibit strong interactions between Al ions and paramagnetic Cu are, at least partially, responsible for the maintenance of higher temperature NH_3 SCR activity. Such Cu/AlO_x structures may be thought of as small, isolated Cu-aluminate-like species which remain dispersed in the intact zeolite channels of the hydrothermally aged Cu-ZSM-5 and Cu-beta catalysts.

4. Conclusions

The effects of hydrothermal aging on the materials properties and NH_3 SCR activity of Cu-ZSM-5, Cu-BEA, Cu-Y, and Cu-SSZ-13 catalysts were studied here. After hydrothermal treatment at 800 °C for 16 h, Cu-SSZ-13 was found to show essentially no change in NO_x reduction activity, while Cu-Y completely lost its NH_3 SCR activity. Both Cu-ZSM-5 and Cu-BEA were found to lose NO_x reduction activity primarily at low temperatures (<350 °C). In the presence of equimolar amounts of NO and NO_2 in the feed gas, significant amounts of N_2O were produced over the aged Cu-ZSM-5 and Cu-BEA at all temperatures.

XRD measurement indicated that the zeolite structure remained largely intact for all the Cu/zeolite catalysts following the hydrothermal aging, except for Cu-Y. When the zeolite framework aluminum species were probed using solid state ^{27}Al-NMR, a significant reduction in the intensities of tetrahedral aluminum peak was observed for the aged Cu-ZSM-5 and Cu-beta catalysts suggesting some de-alumination, while little changes were seen in the spectra for Cu-SSZ-13. ^{27}Al-NMR peaks due to octahedral aluminum ions are expected for the aged and partially de-aluminated zeolite catalysts but were not observed in their spectra. This suggests that paramagnetic Cu ions are strongly interacting with the aluminum ions that are removed from the zeolite framework. When the redox behavior of Cu species was examined using H$_2$-TPR, it was found that Cu^{2+} could be reduced to Cu^{+} and to Cu^{0} in Cu-ZSM-5 and Cu-beta, while Cu^{2+} could be reduced to Cu^{+} only in Cu-SSZ-13. After hydrothermal aging, CuO and Cu-aluminate-like species were found to form in Cu-ZSM-5 and Cu-beta, while little changes were observed for Cu-SSZ-13, consistent with the minor changes in the SCR activity of this latter catalyst.

Acknowledgments

We gratefully acknowledge the US Department of Energy (DOE), Office of Energy Efficiency and Renewable Energy/Vehicle Technologies Program for the support of this work. The research described in this paper was performed at the Environmental Molecular Sciences Laboratory (EMSL), a national scientific user facility sponsored by the DOE's Office of Biological and Environmental Research and located at Pacific Northwest National Laboratory (PNNL). PNNL is operated for the US DOE by Battelle Memorial Institute under contract number DE-AC05-76RL01830.

References

[1] J.H. Lee, M.J. Paratore, D.B. Brown, SAE 2008-01-0072.
[] M. Iwamoto, H. Furukawa, Y. Mine, F. Uemura, S. Mikuriya, S. Kagawa, J. Chem. Soc., Chem. Commun. (1986) 12723.
[3] J.H. Kwak, R.G. Tonkyn, D.H. Kim, J. Szanyi, C.H.F. Peden, J. Catal. 275 (2010) 187.
[4] I. Bull, W.-M. Xue, P. Burk, R.S. Boorse, W.M. Jaglowski, G.S. Koermer, A. Moini, J.A. Patchett, J.C. Dettling, M.T. Caudle, US Patent, 7610,662, 2009.
[5] P.J. Andersen, J. Casci, H.Y. Chen, K. Collier, J.M. Fedeyko, R. Foo, R. Rajaram. In: The 22nd North American Catalysis Society Meeting, June, 2011 (no publication yet).
[6] G. Cavataio, H.W. Jen, J.R. Warner, J.W. Girard, J.Y. Kim, C.K. Lambert, SAE 2008-01-1025.
[7] D.W. Fickel, R.F. Lobo, J. Phys. Chem. C 114 (2010) 1633.
[8] K. Rahkamaa-Tolonen, T. Maunula, M. Lomma, M. Huuhtanen, R. Keiski, Catal. Today 100 (2005) 217.
[9] M. Colombo, I. Nova, E. Tronconi, Catal. Today 151 (2010) 223.
[10] J.Y. Yan, W.M.H. Sachtler, H.H. Kung, Catal. Today 33 (1997) 279.
[11] J.Y. Yan, G.-D. Lei, W.M.H. Sachtler, H.H. Kung, J. Catal. 161 (1996) 43.
[12] E. Bourgeat-Lami, P. Massiani, F. Di Renzo, P. Espiau, F. Fajula, T. Des Courieres, Appl. Catal. 72 (1991) 139.
[13] S.M. Campbell, D.M. Bibby, J.M. Coddington, R.F. Howe, R.H. Meinholdz, J. Catal. 161 (1996) 338.
[14] J.-H. Park, H.J. Park, J.H. Baik, I.-S. Nam, C.-H. Shin, J.-H. Lee, B.K. Cho, S.H. Oh, J. Catal. 240 (2006) 47.
[15] O. Kröcher, M. Devadas, M. Elsener, A. Wokaun, N. Söger, M. Pfeifer, Y. Demel, L. Mussmann, Appl. Catal. B: Environ. 66 (2006) 208.
[16] S. Kieger, G. Delahay, B. Coq, B. Neveu, J. Catal. 183 (1999) 67.
[17] J. Dedecek, B. Wichterlova, P. Kubat, Microporous Mesoporous Mater. 32 (1999) 63.
[18] R. Bulanek, B. Wichterlova, Z. Sobalik, J. Tichy, Appl. Catal. B: Environ. 31 (2001) 3.
[19] J.H. Kwak, R. Tonkyn, D. Mei, S.J. Cho, L. Kovarik, J.H. Lee, C.H.F. Peden, J. Szanyi, ACS Catal., submitted for publication.